APPS/PSNZ Meeting - Sydney 2003

1615 - Poster Communications 1

Monday 29 September 2003

Motor unit discharge properties of respiratory muscles during quiet breathing

J.P. Saboisky, J.E. Butler and S.C. Gandevia, Prince of Wales Medical Research Institute, Randwick, Sydney, NSW 2031, Australia.

The diaphragm is considered the principal muscle of inspiration. However, many other muscles have an inspiratory action with different mechanical linkages to the rib cage. In this study we compared the discharge properties of single motor units in a range of "obligatory" human inspiratory muscles to quantify the distribution of inspiratory neural drive to each of the inspiratory motoneurone pools during quiet tidal breathing.

Studies were performed on 5 healthy volunteer subjects who sat comfortably in an upright chair while breathing through a mouth piece. We recorded single motor unit activity from five separate inspiratory muscles; diaphragm, scalenes, parasternal intercostals, dorsal external intercostals (third space) and dorsal external intercostals (fifth space), during normal quiet breathing (e.g. Gandevia *et al.*, 1999; De Troyer *et al.*, 2003). Electromyography recordings were made from 10 sites within each muscle using monopolar needle electrodes. Each of the muscles were studied on separate occasions. Before each measurement, the thicknesses of the musculature at the sites of intramuscular electrode insertion were assessed using ultrasonography (e.g. De Troyer *et al.*, 1997). Data were sampled and analysed through a commercially available spike-analysis system. Measurements were made of the onset and peak discharge properties of single motor units, and inspiratory flow and were averaged over three breaths.

In total, we recorded from 260 single motor units. The data (mean ± SEM) are summarised in the Table below.

Muscles	**Diaphragm**	**Scalenes**	**Parasternal intercostal**	**Dorsal external intercostal (3^{rd} Space)**	**Dorsal external intercostal (5^{th} Space)**
No. of units	40	57	63	66	34
Onset time (ms)*	377±62	421±73	666±50	637±61	1119±129
Onset time %**	21.7 ± 3.3	21.0 ± 3.4	31.6 ± 2.4	30.4 ± 2.2	41.7 ± 3.8
Onset frequency (Hz)	8.0±0.3	5.9±0.2	7.0±0.6	7.9±0.6	5.9±0.2
Frequency peak (Hz)	12.6±0.5	9.1±0.3	11.8±0.3	12.4±0.4	10.2±0.4

** defined as the time after onset of inspiratory flow.*
*** defined as onset time relative to total inspiratory time.*

The results suggest that there is relatively early recruitment of the diaphragm and scalene muscles. The diaphragm and dorsal external intercostal muscles (third space) had the highest initial (P<0.05) and peak firing frequencies (P<0.01). The data describe for the first time the discharge properties of inspiratory motoneurons from a range of human inspiratory muscles during quiet breathing. It is likely that there is a non-uniform output from the different inspiratory motoneurone pools during quiet tidal breathing.

De Troyer, A., Leeper, J.B., McKenzie, D. K. & Gandevia, S.C. (1997) *American Journal of Respiratory Critical Care Medicine*, **155,** 1335-1340.

De Troyer, A., Gorman, R. B. & Gandevia, S. C. (2003) *Journal of Physiology*, **546,** 943-954.

Gandevia, S. C., Gorman, R. B., McKenzie, D. K. & De Troyer, A. (1999) *American Journal of Respiratory Critical Care Medicine*, **160,** 1598-1603.

Block of the divalent anion channel in the SR of rabbit skeletal muscle by disulfonic stilbene derivatives

K. Bradley and D.R. Laver , School of Biomedical Science, University of Newcastle, Australia.

Previous studies have identified two types of anion channels in the sarcoplasmic reticulum (SR) of rabbit skeletal muscle (Kourie *et al.*, 1996). One of these anion channels has an appreciable anion conductance (saturating at 20pS for phosphate (P_i) and 60pS for SO_4^{2-}). It was proposed that these channels could be responsible for movement of phosphate across the SR membrane (Laver *et al.*, 2001). To further investigate this hypothesis we have searched for specific inhibitors of the divalent anion channel with the rationale that these inhibitors would prevent P_i transport across the SR.

SR vesicles containing the anion channels were isolated from rabbit skeletal muscle that was removed from dead rabbits. Transport of P_i across the SR vesicle membrane was inferred from the P_i assisted component of Ca^{2+} uptake by the SERCa pump. Ca^{2+} uptake was measured from the optical absorbance of antipyrylazo III (Dulhunty *et al.*, 1999). Ca^{2+} uptake experiments were carried out using solutions containing 100 mM KCl or KP_i, 4mM $MgCl_2$, 1mM ATP, 5μM ruthenium red, 0.5 mM antipyrylazo III, 5 mM TES (pH 7). Anion channels were incorporated into lipid bilayers using standard techniques (Laver *et al.*, 2001). Cytoplasmic solutions contained 260 mM Mg^{2+} (250 mM $MgSO_4$ and 10 mM $MgCl_2$), 1 mM $CaCl_2$ 10 mM TES at pH 7.4. Luminal solutions contained 60 mM Mg^{2+} (50 mM $MgSO_4$ and 10 mM $MgCl_2$), 10 mM TES, pH 7.4.

Lipid bilayer studies showed that the divalent anion channels were inhibited by the disulfonated stilbene derivatives, Diisothiocyanostilbene-2',2'-di-sulfonic acid (DIDS), 4,4'-dinitrostilbene-2,2'-disulfonic acid (DNDS), 4,4'-dibenzamidostilbene-2,2'-disulfonic acid (DBDS) and by suramin. Reversible block by these compounds inhibited these channels with high affinity from the cytoplasmic side (~0.1-1μM) and low affinity from the luminal side (0.1 - 1 mM). The voltage-dependent kinetics of drug binding and dissociation indicated that these compounds can dissociate from the channel to either side of the membrane (*i.e.* they are permeant blockers). DIDS also produces non-reversible inhibition of the channel.

Measurements of P_i facilitated calcium uptake by rabbit SR vesicles were used to assay the degree of P_i transport across the SR membrane. The presence of DBDS at concentrations sufficient to block the divalent anion channel in lipid bilayers (~1-10μM) had no effect on P_i transport. Thus it appears that while this channel conducts P_i, it is not the major pathway for P_i in the SR membrane.

Dulhunty, A.F., Laver, D.R., Gallant, E.M., Casarotto, M.G., Pace, S.M. &Curtis, S. (1999) *Biophysical Journal*, **77:**189-203

Kourie, J.I., Laver, D.R., Junankar, P.R., Gage. P.W. & Dulhunty, A.F. (1996) *Biophysical Journal*, **70:**202-221.

Laver, D.R., Lenz, G.K.E., Dulhunty, A.F. (2001) *Journal of Physiology*, **535:**715-728.

Aberrant splicing of ryanodine receptor in myotonic dystrophy

T. Kimura[1,2], M.P. Tkahashi[1] and S. Sakoda[1], [1]Clinical Neuroscience (Neurology), Graduate School of Medicine, Osaka University, Suita, Osaka, Japan. and [2]Present Address: Muscle Research, John Curtin School of Medical Research, Australian National University, Canberra ACT, Australia.
(Introduced by A.F. Dulhunty)

It was reported that mRNAs for chloride channel (Mankodi *et al*., 2002), cardiac troponin T, insulin receptor and myotubularin-related 1 were aberrantly spliced in muscles from myotonic dystrophy (DM). In all cases, the developmentally regulated splice switch that involves a choice between two or more alternative isoforms is skewed, resulting in preferential expression of the isoform that is usually expressed in immature or non-skeletal muscle tissues. We previously reported the induction of the mRNA of small-conductance Ca^{2+}-actvated K^+ (SK3) channel that is usually expressed in immature fibers (Kimura *et al.*, 2000). Taken together, we postulate that there is a maturation-related abnormality in DM that explains the abnormal splicing and transcription. Based on this hypothesis, we investigated the splicing of two candidate mRNAs, which are developmentally regulated.

We used 28 muscle specimens; 10 from myotonic dystrophy type 1 (DM1), 5 from Amyotrophic Lateral Sclerosis, 5 from Polymyositis, 2 from limb-girdle muscular dystrophy and 6 from normal control. Myotubes cultured from 2 muscle specimens; 1 from DM1 and 1 from normal control, were also used. We examined splicing pattern of insulin receptor, ryanodine receptor of skeletal muscle type (RyR1) and β-tropomyosin, using RT-PCR. The total amount of RyR3 mRNA, which is expressed in immature muscles, was quantified. We also employed transgenic mice model of DM1, in which expanded CUG repeat expression in skeletal muscle leads to a DM-like phenotype, for the splicing pattern of RyR1.

We found a significant increase of an alternatively spliced isoform of RyR1 in DM1 patients. The alternative splicing results in the deletion of 5 amino acids at a modulatory region of the receptor and the isoform is normally expressed in undifferentiated muscles. The other splicing isoform of RyR1 was not significantly altered. The splicing of β-tropomyosin and the total amount of mRNA for RyR1 and RyR3 did not differ significantly. In mice, we found a significant increase of the same spliced isoform in long-repeat transgenic mice compared with short-repeat transgenic mice or wild type mice.

The same splicing pattern was found in DM1 patients and DM1 model mice, suggesting that expanded CUG repeat is sufficient for the abnormal splicing. The increase of an immature isoform of RyR1 supports our hypothesis of maturation-related abnormality in DM. Furthermore, RyR1 channel is a major calcium release pathway from sarcoplasmic reticulum and regulate contraction of skeletal muscle. It is possible that the aberrant isoform may be responsible for muscular degeneration of DM, although functional studies for this isoform are needed.

Kimura, T., Takahashi, M.P., Okuda, Y., Kaido, M., Fujimura, H., Yanagihara, T., & Sakoda, S. (2000) *Neuroscience Letters*, 295(3):93-6.

Mankodi, A., Takahashi, M.P., Jiang, H., Beck, C.L., Bowers, W.J., Moxley, R.T., Cannon, S.C., & Thornton, C.A. (2002) *Mollecular Cell*, 10(1):35-44.

Glutathione transferase mu-2 modulation of the activity of muscle sarcoplasmic reticulum

Y.A. Abdellatif, S. Watson, A.F. Dulhunty, P. Board and P.W. Gage, Muscle Research Group, John Curtin School of Medical Research, Australian National University, Mills Road, Acton, Canberra, ACT 2601, Australia.

Glutathione transferases (GST) are versatile enzymes with a wide range of activities ranging from conjugation of glutathione to toxic xenobiotics to maintaining protein disulfi de bonds (Sheehan *et al*., 2001).

Members of the GST family have been shown by our group to affect the activity of both skeletal and cardiac ryanodine receptors (RyR) (Dulhunty *et al*., 2001). The present work focuses on glutathione transferase mu-2 (GST mu-2), one of the major GST isoforms in humans (Van Bladeren *et al*., 2000).

The effects of GST mu-2 on skeletal and cardiac RyRs (isolated from New Zealand rabbit back and hind leg and pig heart respectively) were observed at the single channel level using planar lipid bilayers using symmetrical caesium methansulphonate as current carrier (250/250 mmol/l; *cis* (cytoplasmic*)/trans* (luminal)). $CaCl_2$ (100 μmol/l) was used to activate the channel on the cytoplasmic side at ± 40 millivolt of holding potentials. When GST mu-2 was added to the cytoplasmic side of the skeletal RyR, different effects were observed depending on the holding potential. At +40 millivolt there was a decline in the activity of the channel in a dose dependent manner. Up to approx 80% decrease in the relative mean current (mean current in presence of GST mu-2 compared to control) was observed with 16 μmol/l GST mu-2 (n=8). Further investigation revealed that the effect of GST was voltage dependent (14 out of 16 channels) as at -40 millivolt GST mu-2 signifi cantly activated the channel showing about 3 fold increase in the relative mean current (n=8). In the presence of GST mu-2, cardiac ryanodine receptor showed a decrease in activity at -40 millivolt, the inhibition being more prominent at +40 millivolt. 2 μmol/l GST mu-2 led to approx 40% decrease in the relative mean current at -40 millivolt compared to approx 60% decrease at +40 millivolt (n=6).

The effect of GST mu-2 on calcium induced calcium release and calcium uptake was investigated in skeletal muscle sarcoplasmic reticulum using stopped-flow technique. 8 μmol/l GST mu-2 reduced the rate constant of calcium release by approx 40% (average of 50 traces in 6 experiments) while 10 μmol/l GST mu-2 increased calcium uptake rate constant by approx 13% (average of 40 traces in 6 experiments).

In conclusion (1) GST mu-2 inhibited skeletal RyR at + 40 millivolt while it activated it at 40 millivolt; indicating that GST mu-2 modulation of the skeletal RyR was voltage dependent; (2) GST mu-2 inhibited cardiac RyR, the inhibition being more prominent at positive voltage; (3) GST mu-2 inhibited calcium induced calcium release in skeletal sarcoplasmic reticulum; (4) GST mu-2 potentiated calcium uptake by the skeletal sarcoplasmic reticulum; (5) GST mu-2 effect on calcium release and uptake is potentially a product of the interaction with both the ryanodine receptor and the calcium pump.

Dulhunty, A., Watson, S., Board, P., & Gage, P. 2001. *Journal of Biological Chemistry* 276(5):3319-23.

Sheehan, D., Meade, G., Foley, V.M., & Dowd, C.A. 2001 *Biochemical Journal* 360(Pt 1):1-16.

Van Bladeren, P.J. 2000 *Chemico-Biological Interactions*: 129: 6176.

The effect of prolonged ischemia on the tonic stretch reflex of the tibialis anterior muscle and stiffness of the ankle joint

J.A. Burne and A.R.N.M.H. Haque, School of Biomedical Science, University of Sydney, P0 Box 170, Lidcombe, NSW 2141, Australia. (Introduced by J.M. Lingard)

The aim of this study was to characterise the response of large and small muscle afferents to stretches over the low range of frequencies encountered during normal voluntary movement and to relate these changes to changes in joint stiffness. In 12 normal human volunteers, we elicited tonic stretch reflexes (TSR) in the contracting (10% of maximum voluntary contraction (MVC)) ankle dorsi-flexors using a complex 2min stretch sequence. The sequence contained frequencies spanning 0.1-14 Hz. The stretch was digitally generated and applied by a position-controlled servomotor before, during and after 24.5 min of ischemia produced by inflation of a cuff above the knee. The surface electromyography (EMG), joint angle and resistive torque records were analogue low-pass filtered (400 Hz) and digitised at 1000Hz. Reflex gain and coherence were computed by correlating the rectified and low-pass filtered EMG signals with the record of joint angle. (Matlab V6, Mathworks, USA).

Figure

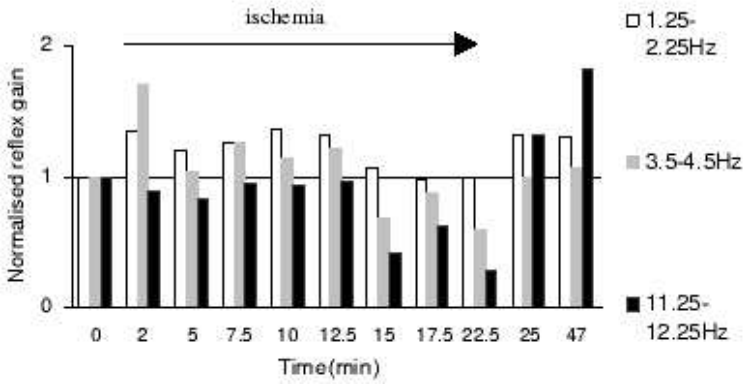

The figure shows relative changes in TSR gain before (time=0), during (2-22.5min) and after (25-47min) ischemia for 3 representative frequency ranges. The gain of the reflex response to the lowest frequencies increased in early ischemia (at 2, 5, 7.5, 10 & 12.5 min) but not significantly (ANOVA, $P>0.05$) in comparison to control values (time=0). The gain of the middle frequency range increased significantly at 2 min of ischemia (ANOVA, $P=0.03$) and then declined during 15 - 22.5 min. The high frequency gain was most sensitive to ischemia. It tended to decline 2 min after cuff inflation and remained significantly decreased at 15 and 22.5 min (ANOVA, $P<0.05$, $P<0.01$) by about 70% of the control value. The high frequency gain showed significant recovery at 0.5 and 22.5 min after cuff deflation (ANOVA, $P=0.002$, $P=0.003$) compared with the last ischemic TSR value.

The resonant frequency (RF) of the ankle joint, calculated from the resistive torque data, increased in a linear manner with contraction of the ankle dorsi-flexors up to 20% of MVC (linear regression analysis, $P<0.00001$) (rest=7.07+1.15 Hz). The RF tended to decrease slightly during ischemia. However, the change was significant only at 2 min (ANOVA, $P=.04$) compared to the control value.

We conclude that both ischemia-sensitive and ischemia-resistant muscle afferents contribute to the stretch response and that they can be distinguished partly through their different stretch frequency responses. The evidence for an association between muscle reflex effects and effects on mechanical joint stiffness was not strong under the experimental conditions.

The effect of background contraction and prolonged ischemia on the tendon reflex

A.R.N.M.H. Haque and J.A. Burne, School of Biomedical Science, University of Sydney, P0 Box 170, Lidcombe, NSW 2141, Australia. (Introduced by J.M. Lingard)

We studied the tendon reflex with the aim of characterising the contributing afferents on the basis of their sensitivity to ischemia. The experiment was done on 12 healthy human volunteers. The left foot was strapped to a foot plate controlled by a servo-motor that could detect force changes about the ankle. Tendon taps were applied to the Achilles tendon with a hammer that was hinged and fell under gravity to deliver a constant blow. A series of 10 responses was recorded at each background contraction of rest, 5%, 10%, 15%, 20% of maximum voluntary contraction (MVC) of the ankle plantar-flexor against the foot plate. Then ischemia was induced in the recorded lower limb by inflation of a blood pressure cuff on the left thigh. Taps were applied to the resting muscle during ischemia at the times shown in the figure and at 2.5 min intervals up to 32.5 min after cuff deflation. Even after our attempts to standardise the delivered taps, we found a large variance within each series of 10 and between subjects. This has been noted earlier (Toft *et al*, 1991). Coefficients of variations (CV) were high at all contraction levels but decreased for the taps applied at 15% and 20% of MVC. Despite the high CVs, the amplitude, when averaged over the series of 10, increased in a highly linear manner with the contraction level (linear regression, $P<0.00001$). This result emulates the effect of contraction level on the tonic stretch reflex gain (Neilson & McCoughy, 1981) but has not been previously observed in tendon reflexes. The tendon reflex amplitude, after normalising for background contraction level, decreased significantly (ANOVA, $P<0.000001$) after 4 min of ischemia to about 50% of the control value and remained depressed throughout the ischemic period. A transient recovery occurred after cuff deflation (ANOVA, $P=.00002$, data not shown in the figure) when compared with the last ischemic tap amplitude but the response remained depressed for the rest of the measured post ischemic period.

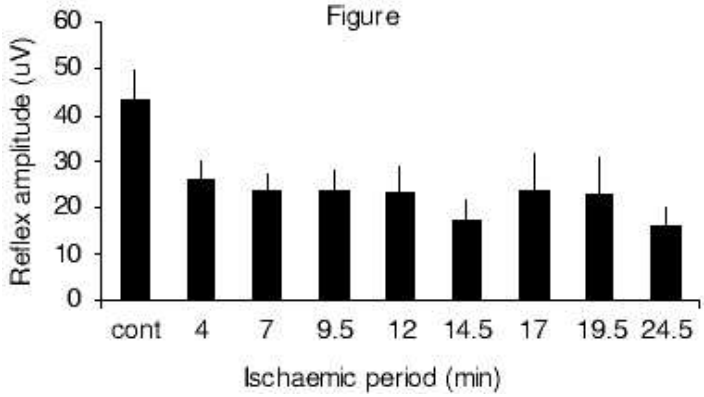

The data indicate that the tendon reflex is mediated by both ischemia- sensitive and ischemia-resistant fibres. The data from the accompanying abstract (Burne & Haque, 2003) suggest that fibres mediating high frequency stretches are more sensitive to ischemia than those mediating low frequencies. Given that taps constitute a broad-band stretch containing frequencies 0.1-100 Hz (data not shown), the high frequency component might be responsible for the quick depression and the low frequency component for the ischemia-resistant component.

Burne, J. & Haque, A. (2003) *Proceedings of Australian Physiological and Pharmacological Society,* **33:**39P.

Neilson, P. & McCoughy, J. (1981) *Journal of Neurology, Neurosurgery and Psychiatry,* **44:** 1007-1012.

Toft, E., Sinkjaer, T. & Rasmussen, A. (1991) *Acta Neurologica Scandinavica,* **84:** 311-315.

Acute incremental exercise, sprint exercise, as well as chronic intermittent hypoxia each decrease muscle Na^+K^+ATPase activity

R.J. Aughey[1], J.A. Hawley[2], C.J. Gore[3], A.G. Hahn[3], D.T. Martin[3], S.A. Clark[2], N.E. Townsend[3], T. Kinsman[3], M.J. Ashenden[3], K.E. Fallon[3], G.J. Slater[3], A.P. Garnham[4], C.M. Chow[5] and M.J. McKenna[1], [1]Centre for Rehabilitation, Exercise and Sports Science, Victoria University of Technology, Melbourne, [2]RMIT University, Melbourne, [3]Australian Institute of Sport, Canberra, [4]Deakin University, Melbourne, and [5]University of Sydney, NSW 2006, Australia.

The Na^+K^+ATPase enzyme is vital in maintaining skeletal muscle excitability. Athletes commonly use hypoxic exposure to improve athletic performance, favouring the live high, train low approach (LHTL). Paradoxically, muscle Na^+K^+ATPase content is reduced by chronic hypoxia (Fraser *et al.*, 2002), which would be expected to reduce muscle performance. Muscle maximal Na^+K^+ATPase activity is also decreased with fatiguing single-leg kicking exercise (Fraser *et al.*, 2002), although the effects of acute intense cycle exercise are unknown. We therefore investigated the effects of acute incremental and sprint exercise and of LHTL on muscle Na^+K^+ATPase activity and exercise performance.

Two studies were performed, where control subjects slept and trained in Canberra (altitude ~600m), whilst the LHTL groups slept in a hypoxic room (study 1, 3000m for 23-nights; study 2, 2650 m for 20-n), and trained at 600m. In study 1, 13 endurance athletes were assigned to either a control (CON, n=6) or LHTL group (n=7). In study 2, 21 endurance athletes were assigned to a control (CON2, n=7), 20 consecutive night LHTL ($LHTL_c$, n=7), or an intermittent 20 night LHTL ($LHTL_i$, 4 x [5-n LHTL then 2-n CON]) group. The lower simulated altitude and intermittent exposure in study 2 were used to reflect common athletic practice. A vastus lateralis muscle biopsy was taken at rest and immediately after incremental exercise prior to (Pre) & after (Post) 23-n of LHTL (study 1); and at rest and immediately after ~1-min sprint exercise prior to (Pre) and after (Post) 20-n LHTL (study 2.) The timecourse of adaptation was investigated in study 2 via an additional rest and post sprint exercise muscle biopsy taken after 5-n of LHTL. Muscle was analysed for maximal *in vitro* Na^+K^+ATPase (K^+ stimulated, 3-*O*-MFPase) activity. Arterialised venous plasma [K^+] was analysed during and following incremental (study 1) and sprint exercise (study 2).

Muscle 3-*O*-MFPase activity was depressed to a similar extent after both incremental (-12.4±0.8%, study 1, exercise effect, $P<0.05$) and sprint exercise (-12.3±0.5%, study 2, exercise effect, $P<0.05$). In study 1, the change in resting 3-*O*-MFPase activity (Pre Post) was greater in LHTL (-2.9±1.1%, $P<0.05$) than CON (0.4±0.5%, NS). In study 2, resting muscle 3-*O*-MFPase was also reduced from Pre to Day 5 in both $LHTL_c$ and $LHTL_i$ groups (-2.1±0.4% and -2.3±0.2% respectively, $P<0.05$), but was unchanged in CON (0.3±0.9%, NS). Resting 3-*O*-MFPase activity (Day 5 Post) was unchanged in $LHTL_c$ and CON (-0.8±0.7% and 0.5±0.6 respectively, NS), but was reversed and increased in $LHTL_i$ (3.5±1.2%). The Pre - Post change in resting 3-*O*-MFPase activity was lowered in $LHTL_c$ (-2.9±0.7%, $P<0.05$), remained unchanged in CON (0.8±1.0%), but tended to increase in $LHTL_i$ (1.1 ± 1.2%). Plasma [K^+] rose with exercise and then declined post-exercise ($P<0.05$) in each study, but was unchanged by LHTL, $LHTL_c$ and $LHTL_i$ (data not shown).

In conclusion, markedly different exercise regimes each acutely depressed skeletal muscle maximal Na^+K^+ATPase activity, with no residual effect evident after 5d recovery. This effect was reproducible, suggesting an obligatory response to heavy exercise. LHTL at 3000m for 23-n, and at 2650m for 20-n each induced only a small reduction in resting Na^+K^+ATPase activity, which was reversed with inclusion of normoxic nightly exposure. In contrast to continuous hypoxic exposure, LHTL caused only a small depression in Na^+K^+ATPase activity. This was insuffi cient to adversely affect muscle performance or plasma K^+ regulation, but may be energetically advantageous and might explain why exercise performance is not impaired with LHTL.

Fraser, S.F., Li, J.L., Carey, M.F., Wang, X.N., Sangkabutra, T., Sostaric, S., Selig, S.E., Kjeldsen, K. & McKenna, M.J. (2002) *Journal of Applied Physiology,* 93, 1650-1659.

Green, H., Roy, B., Grant, S., Burnett, M., Tupling, R., Otto, C., Pipe, A. & McKenzie, D. (2000) *Journal of Applied Physiology,* 88, 634-640.

This work was partially funded by an Australian Research Council SPIRT grant (C00002552).

A simple method for determining regional visual acuity in humans

D.F. Davey[1] and W. Burke[1,2], [1]Department of Physiology and [2]Department of Anatomy & Histology, Institute for Biomedical Research, University of Sydney, NSW 2006, Australia.

Diseases affecting the retina do not create a uniform lesion throughout the retina. It is therefore useful to be able to assess the functioning of small regions of the retina, both for diagnostic reasons and also to monitor the progress of the disease and treatment. The following method was devised specifically to monitor the development, progress and treatment of a condition known as 'macular hole' in which there is detachment of the retina at the fovea. For this reason the regions of retina studied were in the foveal region, but the method could be adapted to any other part of the retina.

Acuity in the vicinity of the fovea was determined at nine positions. Position 0 was centred on the fovea, positions 1-4 were in the outer fovea, positions 5-8 were in the parafovea. They were chosen in order to determine the spread of the macular hole, if it developed, and whether it developed symmetrically. The method of testing was as follows: the subject sat so that the eye being tested was at 57 cm from the screen of a cathode ray tube monitor (280 cm × 210 cm; 1 cm on the screen ≡ 1°), the other eye being covered. If the subject would normally wear corrective spectacles for that working distance, they were worn for the test. Except during a trial, the screen displayed only cross-bars. The subject focussed on the position on the screen corresponding to the point where the cross-bars would intersect. This procedure avoided having a fixation mark in the same place as a letter at position 0. When ready the subject pressed the space bar and a letter flashed on the screen in one of the nine positions. The identification of the letter by the subject was entered into the computer. The duration of the flash (100 ms), being less than the reaction time, prevented identification of the letter subsequent to an eye movement.

The letters used were the following: A, B, C, D, E, F, H, L, O, P, S, T, X, and Z, a set used in many Snellen charts. The font used was Helvetica Bold. The luminance of the letters was 3.1 cd/m^2 against a background luminance of 23.5 cd/m^2, the ambient luminance in the room being about 18 cd/m^2. The choices of letter and of position in which it was flashed were determined randomly. The GNU (Free Software Foundation) C-library *rand()* function was used to generate a pseudo-random selection from the 14 letters of the Snellen character set for each test flash. The same function was used to select the flash position from the nine test positions. The initial size of a letter was 60 point, occupying 1 cm on the screen, i.e. subtending 1^o.

When a letter was identified correctly, the next time a letter was flashed in that position its size was reduced by a factor of $\sqrt{2}$. When a letter was identified incorrectly, the program kept the size unchanged in that position for a further nine trials. After ten trials at one position, if the percentage correct was 70% or less, the size was increased by a factor of $\sqrt{2}$ and ten trials applied with the new size. If the percentage correct was 80% or more, the size of letter was decreased by a factor of $\sqrt{2}$ and ten trials applied with the new size. The aim of this procedure was to determine a letter size that could be identified on 75% of trials. This size was obtained by linear interpolation between the sizes straddling the 75% correct value. This value was taken as a reasonable measure of the acuity at that position. Comparison of the values within the outer foveal and parafoveal permitted assessment of the symmetry of acuity, while comparisons over time using repeated tests allowed changes in acuity to be detected.

ATP acts as both a competitive antagonist and a positive allosteric modulator at recombinant NMDA receptors

A. Kloda[1], J.D. Clements[2], R. Lewis[1] and D.J. Adams[1], [1]School of Biomedical Sciences, University of Queensland, Brisbane, QLD 4072 and [2]Synaptic Dynamics Lab, John Curtin School of Medical Research, Australian National University, Canberra ACT 0200, Australia.

ATP and glutamate are excitatory neurotransmitters in the CNS, and both modulate synaptic plasticity and LTP in hippocampal neurons (Wieraszko and Ehrlich, 1994). NMDA receptors are primarily responsible for the modulatory actions of glutamate, but the mechanisms underlying ATP´s modulatory effects remain uncertain. In the present study, we investigated the effect of ATP on recombinant NR1a+2A and NR1a+2B NMDA receptors expressed in Xenopus oocytes. ATP inhibited currents evoked by low concentration of glutamate. ATP shifted the glutamate concentration-response curve to the right, suggesting a competitive interaction with the agonist binding site. It was a more potent inhibitor at NR1a+2A receptors than at NR1a+2B receptors. The inhibition was voltage-independent indicating that ATP acts outside the membrane electric field. Other nucleotides including ADP, GTP, CTP and UTP inhibited glutamate-evoked currents with different potencies indicating that the inhibition is dependent on the phosphate chain as well as the nucleotide ring structure. Surprisingly, ATP potentiated currents evoked by saturating concentrations of glutamate. At these concentrations, glutamate out-competes ATP at the agonist-binding site. Therefore the potentiation must be due to ATP binding at a separate site, where it acts as a positive allosteric modulator of channel gating. A simple model of the NMDA receptor was constructed, with ATP acting both as a competitive antagonist at the glutamate binding site and as a positive allosteric modulator at a distinct site. The model reproduced all of the main features of the data. Wieraszko, A and Ehrlich, Y.H. (1994)., J. Neurochem.63:1731-1738. This work was funded by ARC Postdoctoral Fellowship awarded to A.K. and ARC Large Grant (A00105778). J.D.C is funded by an ARC Senior Research Fellowship.

Inhibitory synaptic transmission in mouse type A and B medial vestibular nucleus neurones *in vitro*

A.J. Camp, B.A. Graham, R.J. Callister and A.M. Brichta, School of Biomedical Sciences, Faculty of Health, University of Newcastle, Callaghan, NSW 2308, Australia.

The precise roles played by the neurotransmitters GABA and glycine in the maintenance of posture and balance are poorly understood. In the medial vestibular nucleus (MVN) fast inhibitory drive is known to be mediated by $GABA_A$ receptors ($GABA_AR$) and indirect evidence suggests that glycine also plays a role. To directly assess the contribution of $GABA_AR$-mediated and glycine receptor (GlyR) mediated synaptic transmission we recorded miniature inhibitory synaptic currents (mIPSC) in the two major physiological classes (Type A and Type B) of MVN neurones. All experimental procedures were approved by the University of Newcastle Animal Care and Ethics Committee. Transverse brainstem slices (300 µm thick) were prepared from 21-28 day-old mice overdosed with Ketamine (100 mg/kg, i.p.). Whole-cell recordings (-70 mV holding potential) were made at room temperature (23°C) from infra-red visualised MVN neurones using patch electrodes with a CsCl-based internal solution. $GABA_AR$-mediated mIPSCs were isolated in TTX (1 µM), CNQX (10 µM), strychnine (1 µM) and were blocked by bicuculline (10 µM). GlyR-mediated mIPSCs were isolated in CNQX (10 µM), TTX (1 µM), bicuculline (10 µM) and were blocked by strychnine (1 µM). MVN neurones (24/29) received exclusively $GABA_A$ergic, exclusively glycinergic, or mixed mIPSCs (both types). Of the 24 MVN neurones displaying inhibitory events, 10 (42%) received purely $GABA_A$ergic inputs, 3 (12%) received purely glycinergic inputs, and 11 (46%) received Mixed mIPSCs. The rise times of $GABA_A$- and GlyR-mediated mIPSCs were similar for both types of mIPSC (0.7 ± 0.1 ms vs. 0.9 ± 0.5 ms), however the decay time constants for $GABA_A$-mediated events were significantly slower than those for GlyR-mediated events (9.6 ± 1.2 ms vs. 4.3 ± 0.9 ms). Having established that both GABA and glycine are involved in fast inhibitory synaptic transmission in MVN neurones, we next examined if inhibitory drive differed for Type A and Type B neurones. MVN neurones receiving mixed ($GABA_A$ergic and glycinergic) and exclusively glycinergic inputs had higher background discharge rates than those receiving exclusively $GABA_A$ergic inputs (24.1 ± 8.9 Hz n=4 and 9.4 ± 3.4 Hz n=2, respectively vs. 5.4 ± 1.0 Hz n=6). The type of inhibitory input was also correlated with the MVN neurone's physiological class. Using a combination of voltage- and current-clamp recording techniques, our initial results suggest that Type A neurones, which have a monophasic AHP, receive both glycinergic and mixed inhibitory inputs. Type B neurones, which have a biphasic AHP, receive only $GABA_A$ergic inhibitory inputs. These findings show that both GABA and glycine contribute to inhibitory synaptic processing in MVN neurones. Furthermore, inhibition mediated by $GABA_A$Rs and GlyRs may differ in Type A and Type B MVN neurones.

Supported by Hunter Medical Research Institute (HMRI), and the Garnett Passe & Rodney Williams Memorial Foundation.

Ryanodine receptor isoforms in the neonatal rat cochlea

R.T. Whitehead, M.B. Cannell and G.D. Housley, Department of Physiology, Faculty of Medical Health Science, University of Auckland, Private Bag 92019, Auckland, New Zealand.

Intracellular Ca^{2+} plays an essential role in many aspects of cochlear function. The ryanodine receptor (RyR) intracellular Ca^{2+} release channel has been implicated in the regulation of both auditory neurotransmission and sound transduction (Bobbin, 2002; Kennedy and Meech, 2002; Sridhar *et al.*, 1997). Nevertheless, there is a lack of data on the localisation of RyR mRNA and protein in the cochlea.

RyR isoform (RyR1, RyR2, RyR3) mRNAs were amplified from postnatal day 10 rat spiral ganglion neuron (SGN), organ of Corti, and whole cochlea cDNA using the reverse transcription-polymerase chain reaction (RT-PCR) with RyR isoform-specific primers. The identity of the cDNA PCR products was confirmed by sequencing. Ca^{2+} imaging of RyR-mediated Ca^{2+} store release was imaged using 300µm neonatal rat cochlear slices loaded with 10µM fluo 4-AM.

All three RyR isoform mRNA transcripts were detected in the whole rat cochlea and SGN cDNA. However, only RyR1 and RyR3 mRNA transcripts were detected in the organ of Corti. As previously reported, a primary antibody recognising both RyR1 and RyR2 revealed protein expression in the SGN cell bodies and organ of Corti in adult rat cochlea (Whitehead *et al.*, 2002). However, a RyR2-specific antibody showed staining only in the SGN cell bodies, thus the organ of Corti labelling probably reflects RyR1 expression. Functional expression of RyR in the neonatal rat cochlea was confirmed by increases in intracellular Ca^{2+} in the SGN cell bodies and the organ of Corti with bath superfusion of the RyR agonist caffeine (5mM).

This study confirms the expression of multiple RyR isoform mRNA transcripts in the neonatal rat cochlea, and the expression of functional RyR protein in the SGN and organ of Corti. Co-expression of all three RyR isoform mRNA transcripts in the SGN cell bodies suggests a complexity of RyR-mediated Ca^{2+} signalling associated with auditory neurotransmission. The detection of RyR1 and RyR3 mRNA and the immunolabelling for RyR1 in the organ of Corti suggests that both isoforms contribute to regulation of sound transduction.

Bobbin, R.P. (2002) *Hearing Research*, 174: 172-182.
Kennedy, H.J. & Meech, R.W. (2002) *Journal of Physiology*, 539: 15-23.
Sridhar, T.S, Brown, M.C. & Sewell, W.F. (1997) *Journal of Neuroscience*, 17: 428-37.
Whitehead, R.T., Cannell, M.B. & Housley, G.D. (2002) *Proceedings of the Physiological Society of New Zealand*, 21: 29.

Localisation of P2X6 receptor protein expression in the adult rat cochlea

D. Greenwood, L.K. Yang, P.R. Thorne and G.D. Housley, Department of Physiology, University of Auckland, Private Bag 92 019, Auckland 1009, New Zealand.

The P2X6 receptor (P2X6R) is one of seven P2X receptors forming a homologous family of mammalian channel proteins (ATP-gated ion channels). P2X6R cDNA was first isolated from a superior cervical ganglion cDNA library (Collo *et al.*, 1996). mRNA expression of this subtype is highly distributed throughout the brain. There is extensive overlap in localisation of P2X6R mRNA with the other subunits, especially P2X4R and P2X2R, indicating potential for forming heteromeric P2X receptors (Collo *et al.*, 1996). Co expression of P2X6R with P2X2R (King *et al.*, 2000), or P2X4R (Le *et al.*, 1998) can produce modified channel phenotypes whereby the original P2X2R or P2X4R properties are altered, supporting the likely occurrence of P2X6R as a heteromer and extending the functional diversity of these receptors. In the mammalian cochlea extracellular ATP acting at P2X receptors has a major role in auditory function, including sound transduction and auditory neurotransmission. All seven P2XR subunit mRNAs are represented in the cochlea (Greenwood *et al.*, 1999). Previously, P2X6R expression has been localised to the spiral ganglion (Brandle *et al.*, 1999; Xiang *et al.*, 1999). In this study we used immunoperoxidase histochemistry and confocal immunofluoresence to investigate the sites of P2X6R protein expression in adult cochlea. Given the propensity for P2X6R to co localise with P2X2R (Collo *et al.*, 1996) and a recent report demonstrating an up-regulation of P2X2R protein expression in auditory hair cells and spiral ganglion neurones in response to noise (Wang *et al.*, 2003) we investigated whether P2X6R expression was also modified by noise exposure.

Adult Wistar rats were subjected to either ambient noise (control) or white noise at 110dB for 72 hours. Paraformaldehyde fixed cochleae were isolated. Floating 50 mm sections were labelled using a rabbit anti-rat antibody raised against an intracellular C-terminus peptide of the P2X6R coding sequence (Roche, Palo Alto). P2X6R immunoreactivity was detected using a Vectastain Elite ABC kit (Vector Laboratories) and visualised after incubation with the chromogenic substrate 3, 3-diaminobenzidine tetrahydrochloride (Vector Laboratories). A Cy3-conjugated anti-rabbit IgG goat antibody (Chemicon) was utilised as the secondary antibody in the immunofluorescence study. Specificity of the antibody was confirmed by (i) omission of the primary antibody and (ii) with a peptide block of the P2X6R epitope. Intensity of fluorescent P2X6R labelling was analysed using Image Pro Plus software (Adobe).

In this study, the spiral ganglion was confirmed as the principal site of P2X6R expression. Other notable structures showing P2X6R expression included supporting cells of the organ of Corti, and the stria vascularis. P2X6R protein expression was unchanged by noise exposure unlike P2X2R, a potential co-subunit. This finding suggests that P2X6R expression may contribute to heteromultimeric assembly with other P2XR in the cochlea. Possible phenotype modulation conferred by P2X6R may be diminished by noise-induced up-regulation of co-assembled P2XR.

Brandle, U., Zenner, H.P. & Ruppersberg, J.P. (1999) *Neuroscience Letters,* 273: 105-108.

Collo, G., North, R.A., Kawashima, E., Merlopich, E., Neidhart, A., Surprenant, A. & Buell, G. (1996) *Journal of Neuroscience,* 16: 2495-2507.

Greenwood D., Burrows M., Kanjhan R., Raybould N.P., Salih S.G. & Housley G.D. (1999) *Proceedings of the Physiological Society of NZ,* 18: 55p.

King, B.F., Townsend-Nicholson, A., Wildman, S.S, Thomas, T., Spyer, K.M. & Burnstock, G. (2000) *Journal of Neuroscience,* 20: 4871-4877.

Le, K.T., Babinski, K. & Seguela, P. (1998) *Journal of Neuroscience,* 18: 7152-7159.

Wang J.C.C., Raybould N.P., Lin L., Ryan A.F., Cannell M.B., Thorne P.R. and Housley G.D. (2003) *NeuroRepor,t 14(6:) 817-23.*

Xiang, Z., Bo, X. & Burnstock, G. (1999) Hearing Research, 128 190-196.

Studies approved by University of Auckland Animal Ethics Committee. Funded by: Health Research Council, Marsden Fund, Maurice and Phyllis Paykel Trust. I. Oglesby at Roche Palo Alto is thanked for supplying the P2X6 antisera

$GABA_A$ receptor subunit composition in cultured hippocampal neurons from newborn rats

N. Ozsarac[1], M.L. Tierney[2] and P.W. Gage[1], [1]John Curtin School of Medical Research, Australian National University, PO Box 334, Canberra, ACT 2601 and [2]School of Biochemistry & Molecular Biology, Faculty of Science, Australian National University, Canberra, ACT 2601, Australia.

$GABA_A$ receptors are the major inhibitory neurotransmitter receptors in the central nervous system. These heteromeric receptors are composed of five subunits and so far six, α-, three β-, three γ-, one δ-, one ε-, one π- and one θ- subunit have been identified in the mammalian nervous system. A number of pharmacologically important drugs such as benzodiazepines, barbiturates, anaesthetics and convulsants produce at least part of their clinically relevant effects by directly binding to $GABA_A$ receptors. These drugs exert their effects by changing channel kinetics or channel conductance, or both. The generally reported conductance for synaptic $GABA_A$ receptors is 25-30 pS. We have reported much higher conductances of up to 100 pS, and an increase in conductance in the presence of some of the above drugs, in cultured hippocampal neurons from newborn rats (Eghbali *et al.*, 1997). A possible reason for the discrepancy between our results and those of some others is that cultured neurons from newborn rats may have an unusual complement of subunits. Our aim is to identify the subunit composition of $GABA_A$ receptors in these neurons by reverse transcriptase PCR (RT-PCR) in seven-day-old hippocampal cultures from newborn Wistar rats. In initial work, we are concentrating on the main subunits: α, β, γ and δ. Our preliminary results show an absence or a very low quantity of α-1 and 6, β-2, γ-2 and -3 in these cultured cells.

Eghbali, M., Curmi, J.P., Birnir, B. & Gage, P.W. (1997) *Nature,* 388:71-75.

Affinity purification of the skeletal muscle ryanodine receptor using a gluthatione-S-transferase-FKBP12 fusion protein

P. Pouliquin, S. Pace and A.F. Dulhunty, Muscle Research Group, John Curtin School of Medical research, Australian National University, Mills Road, Acton, ACT 2601, Australia.

Calcium is the most ubiquitous second messenger. In numerous cell types, the calcium release channel ryanodine receptor (RyR) plays a central role in calcium signalling. This channel is associated with a plethora of proteins in the cell, and constitutes the core of a supra-macromolecular complex which integrates cell signals and translates them into a calcium signal. In the heart and in the skeletal muscle, RyRs associated with their co-/accessory proteins are central to the excitation-contraction process which is still not fully understood at the molecular level. A better understanding of this critical step and, by extension, of the calcium signalling in many cell types requires better knowledge of the mechanisms which determine the ryanodine receptor function, *via* improved structure-function studies. The most precise studies of ryanodine receptor function are based on single channel recordings after incorporation of the RyR into planar lipid bilayers. Unfortunately, purity of the channel used in those experiments has not been adequate to determine RyR's intrinsic properties. Most studies have been done with microsomal vesicles enriched in RyR. The so called purified receptor contains significant contamination by several proteins. When RyR has been exogenously expressed in cells which don't express it endogenously, the extent of the channel's association with other proteins is not known. Determination of the channel's intrinsic properties and of the precise influence of its numerous co-/accessory proteins requires functional studies performed with pure RyR.

FKBP12 is a small protein which associates tightly with the RyR (Mackrill *et al.,* 2001). We have expressed a GST-FKBP12 fusion protein and used it to perform affinity purification of the RyR from rabbit skeletal muscle isolated after animals had been euthanased by captive bolt. The procedure has been described with few modifications (Mackrill *et al.,* 2001). Heavy sarcoplasmic vesicles were solubilised with 3-[(3-cholamidopropyl)-dimethylamino]-1-propanesulfonate in the presence of phosphatidylcholine. Non solubilised proteins were eliminated by ultracentrifugation; supernatant was then incubated with GST-FKBP12 fusion proteins immobilised on agarose beads. Unbound and unspecifically bound material was removed by successive washes. Purity of the purified ryanodine receptor and yield of the protein were estimated by silver nitrate staining of SDS-PAGE and colorimetric assay, respectively. Attempt to release RyR from the beads-fusion protein complex by the drug rapamycin failed. The ryanodine receptor-fusion protein complex was released from the beads by glutathione, and the excess of fusion protein eliminated by gel filtration. The RyR was purified virtually to homogeneity, the main usual contaminants (calsequestrin and Ca^{2+}-ATPase) not being detected on silver nitrate. Yield of the purified RyR from the heavy sarcoplamic vesicles was estimated close to 60%.

Intrinsic functional properties of the purified protein will be studied using single channel recordings and ^{3}H-ryanodine binding assays. We are also expressing some RyR's co-/accessory proteins as fusion proteins with tags allowing their affinity purification. Addition of those purified co-/accessory proteins to the buffer bathing the purified channel should allow us to explore their regulatory effects on the receptor.

Mackrill, J.J., O'Driscoll, S., Lai, S.F.A., & McCarthy, T.V. (2001) *Biochemical and Biophysical Research Communications* **285,** 5257.

The role of the Ether-à-go-go K^+ channel in cellular proliferation in the mouse preimplantation embryo

S.L. Jones and M.L. Day, Department of Physiology and Institute for Biomedical Research, University of Sydney, NSW 2006, Australia.

The initiation of cell division is a complex process that is currently thought to depend on changes in membrane ion permeability, especially that resulting from K^+ channel activity (Amigorena *et al.*, 1990; Wonderlin and Strobl, 1996). Furthermore, K^+ channel expression and activity (Day *et al.*, 1993; Amigorena *et al.*, 1990) have also been found to be modulated during the cell cycle, which may suggest a novel, non-excitable K^+ channel function: the regulation of cell cycle progression. Ether-à-go-go (*eag*) is a voltage-activated K^+ channel, thought to be involved in cell proliferation (Brüggemann *et al.*, 1997; Pardo *et al.*, 1998).

This study aims to examine the cell cycle dependent expression of *eag* in MCF-7 and trophoblast stem cell lines and determine the extent to which *eag* alters the membrane potential in a cell cycle dependent manner. The expression and potential change will also be examined during development of the mouse preimplantation embryo.

The effects of loss of *eag* expression on membrane potential and cell division will also be examined by specific downregulation of the gene using RNA interference. A plasmid vector will be employed to synthesise siRNA homologous to *eag* mRNA within the cells resulting in degradation of the *eag* mRNA transcript.

These methods may allow a greater understanding of the cell cycle regulated expression of *eag* and the impact of this on changes in membrane potential and the proliferative response.

Amigorena, S., Choquet, D., Teillaud, J., Korn, H. & Fridman, W.H. (1990) *The Journal of Immunology,* **144:** 2038-2045.

Wonderlin, W.F. & Strobl, J.S. (1996) *Journal of Membrane Biology,* **154:** 91-107.

Day, M.L., Pickering, S.J., Johnson, M.H. & Cook, D.I. (1993) *Nature,* **365:** 560-562.

Brüggemann, A., Stühmer, W. & Pardo, L.A. (1997) *Proceedings of the National Academy of Sciences of the USA,* **94:** 537-542.

Pardo, L.A., Brüggemann, A., Camacho, J. & Stühmer, W. (1998) *The Journal of Cell Biology,* **143:** (3) 767-775.

The Cys-loop's role in ligand-binding and channel-gating in the $GABA_A$ receptor

V.A.L. Seymour[1], T. Luu[1], M.L. Tierney[2] and P.W. Gage[1], [1]Department of Molecular Biosciences, John Curtin School of Medical Research, Building 54 - ANU, Mills Rd, Acton ACT 0200 and [2]Biochemistry and Molecular Biology, Faculty of Science, Building 41 - ANU, Linnaeus Way, Acton ACT 0200, Australia.

The Cys-loop is conserved amongst members of the ligand-gated ion channel (LGIC) family. Within this loop there is a conserved motif referred to as the XPZD motif which sits at the bottom of the Cys-loop at positions 8 to 11 where the conserved cysteines are designated positions 1 and 15. The 4 residues that comprise the XPZD motif in the $GABA_A$ receptor are either conserved throughout the LGIC family or the chemical nature of the residue is conserved. The recently solved crystal structure of an acetylcholine binding protein places the Cys-loop at the junction between the extracellular ligand-binding and transmembrane domains (Brejc *et al*., 2001). We hypothesise that the Cys-loop may play a role in linking ligand-binding to channel-gating in the $GABA_A$ receptor. To test this hypothesis we are mutating residues in the conserved XPZD motif within the Cys-loop of $GABA_A$ receptor subunits and examining their ability to function as ion channels.

Mouse L929 cells were transfected with combinations of wild type (WT) ($\alpha1\beta1\gamma2s$) and mutant GABA subunit cDNAs. When the invariant proline residue in the Cys-loop was replaced with alanine (P9′A) in the α or β subunit and co-expressed with the remaining WT subunits, the whole cell response to GABA was reduced. The reduced response could be caused by fewer receptors in the membrane as a result of lower expression, impaired assembly or defective trafficking of receptors or the reduction could be a result of changes in channel properties such as kinetics. To determine the cause of the reduced response, immunofluorescence and radioactive muscimol binding studies are being used to quantitate and compare the presence of mutant receptors in the membrane with the WT receptor and secondly, single channel currents are being recorded to examine if the reduced response is caused by changes in channel kinetics.

The response of $GABA_A$ receptors to agonists can be potentiated by drugs such as diazepam, pentobarbitone and etomidate. The effects of these drugs were tested on $GABA_A$ receptor mutants and compared with the effects on WT $GABA_A$ receptors. Responses were generated with 1μM GABA followed by potentiation with 1μM diazepam, 100 μM etomidate or 50 μM pentobarbitone. The potentiated response to each drug was less than the WT response when proline was mutated to alanine at 9′ in the Cys-loop in either α or β subunits.

The (P9′A) mutation in the Cys-loop of $GABA_A$ subunits reduces the whole cell current in response to GABA and changes responses to various drugs. Further studies are being undertaken to test the role of the Cys-loop in these fundamental actions of the ion channel.

Brejc, K., van Dijk, W. J., Klaassen, R.V., Schuurmans, M., van Der Oost, J., Smit, A.B. & Sixma, T.K. (2001) *Nature,* **411,** 269-276.

Expression of calcium release channels in rat arteries

T.H. Grayson and C.E. Hill, Division of Neuroscience, John Curtin School of Medical Research, Australian National University, Canberra, ACT 0200, Australia.

Changes in intracellular calcium concentration, as a consequence of the regulated opening and closing of Ca^{2+} channels, controls many cellular responses. In arteries, Ca^{2+} released from intracellular stores in smooth muscle cells can cause vasoconstriction or vasodilation, depending on the signaling pathways and calcium sources that are involved (see Hill *et al*., 2001). Similarly, in the endothelium Ca^{2+} released from IP3-sensitive stores is associated with vasodilation but the contribution of other Ca^{2+} sources is unknown. Responses to Ca^{2+} fluxes are coordinated through the endothelium and smooth muscle via gap junctions composed of connexins (Cxs). Differential distribution of Ca^{2+} release channels and Cx subtypes may underlie the variability in responses observed between functionally distinct vessels. We used real-time PCR to examine the subtype-specific expression of mRNA for the inositol 1,4,5-trisphosphate receptor (IP3R), ryanodine receptor (RyR), transient receptor potential channels (TrpC), and vascular Cx isoforms in thoracic aorta (ThA), mesenteric (MA) and basilar (BA) arteries removed from juvenile (14-17 day) and adult (9-13 week) Wistar rats that had been anaesthetised with ether and decapitated (Animal Experimentation Ethics Committee, ANU).

IP3R1 was the most abundantly expressed IP3R subtype in all arteries. Compared with the juvenile, the expression of IP3R1 was increased in the adult ThA but not in other arteries, and the expression of IP3R2 and IP3R3 was reduced in the adult MA and BA.

RyR2 was the predominantly expressed RyR subtype in all arteries. RyR3 was detected at a low level in each artery except in the MA where it constituted 25% of RyR expression. Compared with the juvenile, RyR2 was more abundant in the adult ThA but there were no other significant changes with development. RyR1 was not detected in any artery.

TrpC1 was the predominant TrpC channel in all arteries and, compared with the juvenile, was more abundant in the adult ThA. TrpC3 was mainly expressed in the BA and MA, while TrpC4 was mainly expressed in the MA. TrpC6 expression was at a relatively low level in each artery and was much reduced in the adult. TrpC2, TrpC5 and TrpC7 were not detected in any artery. No other substantial changes were found during development.

The expression of vascular Cxs showed that Cx43 >> Cx37 > Cx40 > Cx45 in the ThA while Cx37 >> Cx40 ≈ Cx45 > Cx43 in the MA and BA. Relative levels of Cx expression did not change substantially between the juvenile and adult, although Cx40 expression was significantly reduced in the adult BA and Cx43 was significantly increased in the adult ThA.

The pattern of expression for IP3Rs was similar amongst the 3 arteries however there were differences between elastic (ThA) and resistance (BA, MA) arteries in the expression of TrpC3 and Cxs. Furthermore, MA was distinguished by the expression of TrpC4 and RyR3. Using subtype-specific antibodies we have recently shown that IP3R1 was found in vascular smooth muscle and endothelium while IP3R2 and IP3R3 were almost exclusively restricted to the vascular endothelium (Grayson *et al*., 2003). Future work will determine whether protein expression and distribution of the other Ca^{2+} channel subtypes varies in a similar manner.

Hill, C.E., Phillips, J.K. &Sandow, S.L. (2001) *Medical Research Reviews*, 21:1-60.

Grayson, T.H., Haddock, R.E., Murray, T.P., Wojcikiewicz, R.J.H. & Hill, C.E. (2003) *ANZMS 11th Symposium Abstracts*, Fraser Island, Queensland, Australia, 11-14 September.

Mineralocorticoid activates epithelial sodium channel via exocytosis in mouse renal collecting duct cells

Y. Hosoda[1], M. Pedler[2], H. Hu[1], A. Beesley[1], C. Bailey[2], A. Dinudom[1], J.E.J. Rasko[2] and D.I. Cook[1], [1]Department of Physiology, University of Sydney, NSW 2006 and [2]Centenary Institute of Cancer Medicine &;Cell Biology, &;Sydney Cancer Centre, Newtown, NSW 2042, Australia.

The epithelial sodium channel (ENaC) plays a critical role in regulating body sodium and fluid homeostasis. Activity of ENaC is regulated by hormones such as aldosterone and insulin. Aldosterone increases ENaC activity within 30 min and this early effect of the hormone is non-genomic. Although the mechanisms that underlie the early effect of aldosterone on ENaC activity are still unknown, it is believed that this effect may be mediated by increasing insertion of ENaC from a cytosolic pool into the cell membrane. To investigate this hypothesis, we used a retroviral expression system and Ussing chamber technique to study regulation of ENaC activity in the mouse collecting duct (M1) cell line. To investigate insertion of ENaC, a glycine codon in the amiloride-sensitive region of the γENaC gene was mutated to cysteine (G542C). A retrovirus expressing this gene was constructed and used to stably transfect M1 cells. The M1 cells that were transfected with G542CγENaC were selected using neomycin resistance and then cultured on Millicell-CM for 14-16 days until the transmembrane resistance was fully developed. The Ussing chamber method was used to measure equivalent short circuit current (Iesc) across the monolayer. The G542C mutation makes ENaC sensitive to [2-(trimethylammonium) ethyl] methanethiosulfonate bromide (MTSET). MTSET forms a disulfide bond with cysteine and inhibits ENaC activity irreversibly. Recovery rate of the MTSET-sensitive current was then used to measure the rate of insertion of active ENaC into the cell membrane.

One hour before each experiment, 100 nM dexamethasone was added to the culture medium. Application of MTSET to the apical side of the monolayers decreased Iesc from 13.0 ± 0.8 to 2.6 ± 0.1μA/cm^2 (n=10). Dexamethasone significantly increased baseline MTSET-sensitive Iesc from 10.3 ± 0.8 μA/cm^2 (n=10) to 19.1 ± 1.2 μA/cm^2 (n=9, P<0.01). After the maximum inhibitory effect of MTSET was observed, the chamber was perfused with HEPES solution for 45 minutes and the slope of MTSET-sensitive Iesc was measured (A in Figure). The slope measured in the dexamethasone treated group (3.8 ± 0.2 nA/cm^2/s) was significantly higher than that of the control group (2.1 ± 0.1 nA/cm^2/s) (B in Figure, P<0.001). The second MTSET sensitive Iesc recovered to 50% of original MTSET sensitive Iesc in both control and dexamethasone groups. Our study, therefore, clearly indicates that the early effect of dexamethasone on Na^+ transport in M1 cells is mediated by increasing insertion of ENaC into the cell membrane.

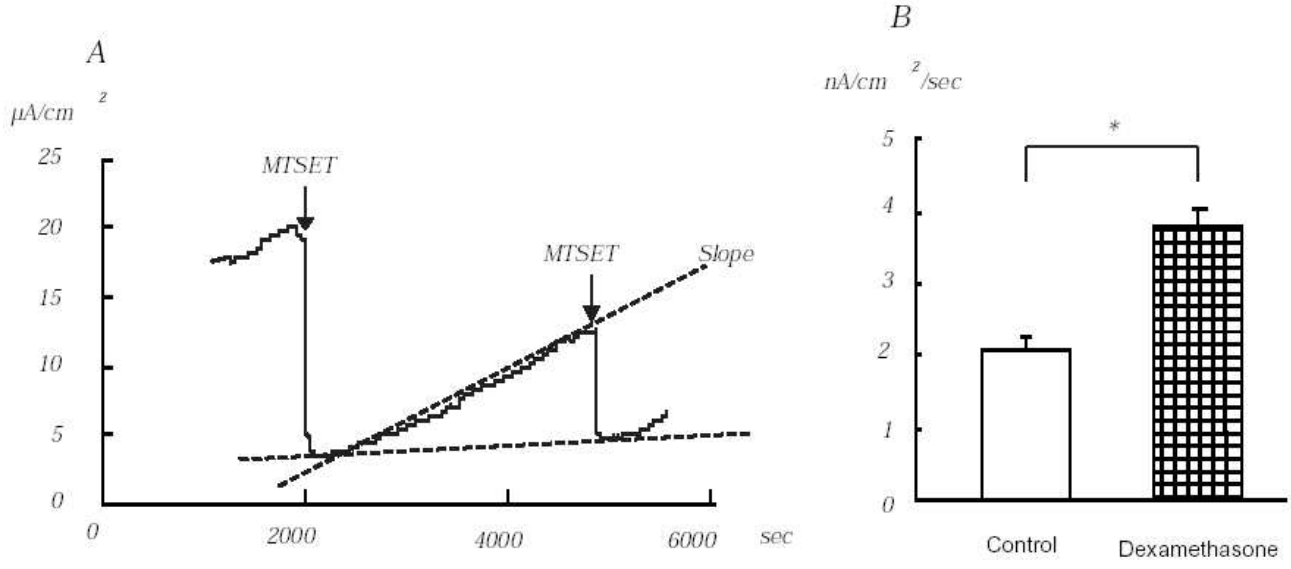

*Inhibition of equivalent short circuit current on M1 cells by MTSET. A: representative trace for change of equivalent short circuit current. MTSET was applied to the apical side only. B: the comparison of slopes between control (n = 10) and dexamethasone treated group (n = 9). * < 0.001.*